



## Iodide substitution in lithium borohydride, $\text{LiBH}_4\text{-LiI}$

Line H. Rude<sup>a</sup>, Elena Groppo<sup>b</sup>, Lene M. Arnbjerg<sup>a</sup>, Dorthe B. Ravnsbæk<sup>a</sup>, Regitze A. Malmkjær<sup>a</sup>, Yaroslav Filinchuk<sup>a,c,d</sup>, Marcello Baricco<sup>b</sup>, Flemming Besenbacher<sup>e</sup>, Torben R. Jensen<sup>a,\*</sup>

<sup>a</sup> Center for Materials Crystallography, Interdisciplinary Nanoscience Center and Department of Chemistry, Aarhus University, Langelandsgade 140, DK-8000 Aarhus C, Denmark

<sup>b</sup> Dipartimento di Chimica I.F.M. and NIS, Università di Torino, Torino, Italy

<sup>c</sup> Swiss-Norwegian Beam Lines at ESRF, BP-220, 38043 Grenoble, France

<sup>d</sup> Institute of Condensed Matter and Nanosciences, Université Catholique de Louvain, Place L. Pasteur 1, B-1348 Louvain-la-Neuve, Belgium

<sup>e</sup> Interdisciplinary Nanoscience Center (iNANO) and Department of Physics and Astronomy, Aarhus University, DK-8000 Aarhus C, Denmark

### ARTICLE INFO

#### Article history:

Received 6 March 2011

Received in revised form 3 May 2011

Accepted 9 May 2011

Available online 1 June 2011

#### Keywords:

Hydrogen storage

Lithium borohydride

Anion substitution

*In situ* powder X-ray diffraction

Sieverts method

Infrared spectroscopy

### ABSTRACT

The new concept, anion substitution, is explored for possible improvement of hydrogen storage properties in the system  $\text{LiBH}_4\text{-LiI}$ . The structural chemistry and the substitution mechanism are analyzed using Rietveld refinement of *in situ* synchrotron radiation powder X-ray diffraction (SR-PXD) data, attenuated total reflectance infrared spectroscopy (ATR-IR), differential scanning calorimetry (DSC) and Sieverts measurements. Anion substitution is observed as formation of two solid solutions of  $\text{Li}(\text{BH}_4)_{1-x}\text{I}_x$ , which merge into one upon heating. The solid solutions have hexagonal structures (space group  $P6_3mc$ ) similar to the structures of *h*- $\text{LiBH}_4$  and  $\beta\text{-LiI}$ . The solid solutions have iodide contents in the range  $\sim 0\text{--}62$  mol% and are stable from below room temperature to the melting point at  $330^\circ\text{C}$ . Thus the stability of the solid solutions is higher as compared to that of the orthorhombic and hexagonal polymorphs of  $\text{LiBH}_4$  and  $\alpha\text{-}$  and  $\beta\text{-LiI}$ . Furthermore, the rehydrogenation properties of the iodide substituted solid solution  $\text{Li}(\text{BH}_4)_{1-x}\text{I}_x$ , measured by the Sieverts method, are improved as compared to those of  $\text{LiBH}_4$ . After four cycles of hydrogen release and uptake the  $\text{Li}(\text{BH}_4)_{1-x}\text{I}_x$  solid solution maintains 68% of the calculated hydrogen storage capacity in contrast to  $\text{LiBH}_4$ , which maintains only 25% of the storage capacity after two cycles under identical conditions.

© 2011 Elsevier B.V. All rights reserved.

### 1. Introduction

One of the greatest challenges of this century is the implementation of an efficient energy storage system which is mandatory in a sustainable, carbon free energy system based on *e.g.* wind and solar energy sources characterised by huge temporal fluctuations. Hydrogen is considered a promising energy carrier for storage of renewable energy having a specific energy content of 120 MJ/kg, which is almost three times higher than that of gasoline (43 MJ/kg) [1,2].

Metal borohydride materials are receiving increasing interest as potential hydrogen storage materials due to their high volumetric and gravimetric hydrogen densities, *e.g.* lithium borohydride,  $\text{LiBH}_4$ , containing  $\rho_v = 122.5 \text{ kg H}_2/\text{m}^3$  and  $\rho_m = 18.5 \text{ wt\% H}_2$  [3–5]. However, important physical properties need to be improved, *e.g.*

due to high thermal stability, hydrogen release and uptake occur only at unfavourable conditions and the kinetics are often too slow. These challenges have been addressed in several ways, such as design of novel bi-metal borohydrides [6–13], utilization of new reaction pathways (reactive hydride composites) [14–17], and the concept of nanoconfinement, where metal hydrides are infiltrated in nano-porous materials [18,19]. Recently, the concept of anion substitution in borohydrides, *e.g.* halide ion substitution of the complex anion  $\text{BH}_4^-$  in  $\text{LiBH}_4$  and  $\text{Ca}(\text{BH}_4)_2$  was investigated regarding crystal structures [20–24] and lithium ion conductivity [25,26]. The ion conductivity in  $\text{LiBH}_4$  is significantly improved for the solid solutions  $\text{LiBH}_4\text{-LiX}$ ,  $\text{X} = \text{Cl, Br, I}$ , and may find applications as solid electrolytes for all-solid-state batteries [25–30]. Fast dissolution of  $\text{LiCl}$  in the hexagonal phase *h*- $\text{LiBH}_4$ , forming *h*- $\text{Li}(\text{BH}_4)_{0.6}\text{Cl}_{0.4}$  at  $240^\circ\text{C}$ , and slow segregation of  $\text{LiCl}$  from the solid solution forming orthorhombic *o*- $\text{Li}(\text{BH}_4)_{0.9}\text{Cl}_{0.1}$  after months at room temperature (*RT*) has been reported [20]. However, only little is known about the rehydrogenation properties of these materials, a subject where anion substitution might have a significant effect.

In this study we focus on the iodide substitution in lithium borohydride. Lithium borohydride exhibits interesting structural chemistry with four known polymorphs [3,31–33], whereof two exist under ambient pressures. The stable *RT* polymorph is

\* Corresponding author. Tel.: +45 8942 3894; fax: +45 8619 6199.

E-mail addresses: [line@inano.au.dk](mailto:line@inano.au.dk) (L.H. Rude), [elena.groppo@unito.it](mailto:elena.groppo@unito.it) (E. Groppo), [lenem@chem.au.dk](mailto:lenem@chem.au.dk) (L.M. Arnbjerg), [inadr@inano.au.dk](mailto:inadr@inano.au.dk) (D.B. Ravnsbæk), [regitze.aagaard.malmkjær@post.au.dk](mailto:regitze.aagaard.malmkjær@post.au.dk) (R.A. Malmkjær), [Yaroslav.Filinchuk@uclouvain.be](mailto:Yaroslav.Filinchuk@uclouvain.be) (Y. Filinchuk), [marcello.baricco@unito.it](mailto:marcello.baricco@unito.it) (M. Baricco), [fbe@inano.au.dk](mailto:fbe@inano.au.dk) (F. Besenbacher), [trj@chem.au.dk](mailto:trj@chem.au.dk) (T.R. Jensen).

**Table 1**  
The composition of the investigated samples is given as the molar ratios and as the molar fractions,  $n(\text{LiI})/n(\text{total})$ , and the hydrogen content,  $\rho_{\text{m}}(\text{H}_2)$ , is calculated. The preparation methods are either ball milling (BM), in two cases followed by annealing (A) in argon atmosphere, or hand-mixing in a mortar (HM).

| Notation   | Materials              | Molar ratio | $n(\text{LiI})/n(\text{total})$ | Preparation           | $\rho_{\text{m}}(\text{H}_2)$ |
|------------|------------------------|-------------|---------------------------------|-----------------------|-------------------------------|
| <b>S1</b>  | LiBH <sub>4</sub> –LiI | 1:0.5       | 0.334                           | BM                    | 3.41                          |
| <b>S1A</b> | LiBH <sub>4</sub> –LiI | 1:0.5       | 0.335                           | BM and A <sup>a</sup> | 3.41                          |
| <b>S2</b>  | LiBH <sub>4</sub> –LiI | 1:0.6       | 0.371                           | BM                    | 3.01                          |
| <b>S2A</b> | LiBH <sub>4</sub> –LiI | 1:0.6       | 0.371                           | BM and A <sup>b</sup> | 3.01                          |
| <b>S3</b>  | LiBH <sub>4</sub> –LiI | 1:1         | 0.500                           | BM                    | 1.94                          |
| <b>S4</b>  | LiBH <sub>4</sub> –LiI | 1:1         | 0.500                           | HM                    | 1.94                          |

<sup>a</sup> 280 °C/96 h.

<sup>b</sup> 245 °C/96 h.

orthorhombic *o*-LiBH<sub>4</sub> with space group symmetry *Pnma* (*no.* 62). At  $T \sim 112$  °C a transformation to the high-temperature hexagonal *h*-LiBH<sub>4</sub> polymorph occurs [31,32,34]. The *h*-LiBH<sub>4</sub> has the space group symmetry *P6<sub>3</sub>mc* (*no.* 186) and is stable until melting at  $T \sim 268$  °C with decomposition of the melt at  $\sim 467$  °C [6,7].

Lithium iodide,  $\alpha$ -LiI, has a cubic NaCl-type structure with space group *Fm-3m* (*no.* 225), in which the Li and I coordinations are octahedral. However, if the ionic radii are considered, Li and I would be expected to exhibit tetrahedral coordination at RT, due to the low ratio between the ionic radii,  $r(\text{cation})/r(\text{anion})$  of 0.25. This is observed in the hexagonal form of LiI, denoted  $\beta$ -LiI, with space group *P6<sub>3</sub>mc* (*no.* 186) that exists at  $T < 0$  °C using a substrate to initiate crystal growth [35–39]. Furthermore, a solid solution of LiI and LiBr can stabilize the  $\beta$ -LiI structure up to 80 °C [35]. The *h*-LiBH<sub>4</sub> and  $\beta$ -LiI therefore obtain a similar structure.

Here we present the synthesis, crystal structure and physical properties of iodide-substituted lithium borohydride investigated by *in situ* synchrotron radiation powder X-ray diffraction (SR-PXD), attenuated total reflectance infrared spectroscopy (ATR-IR), differential scanning calorimetry (DSC) and the Sieverts method.

## 2. Experimental

Samples were prepared using lithium borohydride, LiBH<sub>4</sub> (95%, Aldrich) and lithium iodide, LiI (99.99%, Aldrich) in compositions 1:0.5 (denoted **S1**), 1:0.6 (**S2**) and 1:1 (**S3**). All samples were ball-milled in a Fritch Pulverisette no. 4 using the same procedure, i.e. high energy ball milling under inert conditions (argon atmosphere) comprised of 60 times 2 min of milling each intervened by 2 min breaks to avoid heating of the sample. The sample to ball mass ratio was 1:40 and tungsten carbide (WC) vial (80 mL) and balls (10 mm) were used. A fraction ( $\sim 0.5$  g) of samples prepared in the same way as **S1** and **S2** was transferred to corundum crucibles, placed in sealed argon-filled quartz tubes and annealed (A) in a furnace kept at a fixed temperature of 280 °C (**S1A**) or 245 °C (**S2A**) for 96 h. The samples obtained after annealing are denoted **S1A** and **S2A**, respectively. A sample of LiBH<sub>4</sub>–LiI in composition 1:1 was prepared by hand-mixing (HM) in an agate mortar (denoted **S4**). All investigated samples are listed in Table 1. All sample preparations and handling were performed under inert argon atmosphere in an MBraun Unilab glove box with a recirculation gas purification system and gas/humidity sensors. Oxygen and water levels were kept well below 1 ppm during all operations.

In-house powder X-ray diffraction (PXRD) data were collected at RT using a SuperNova diffractometer (Oxford diffraction) with microfocus MoK $\alpha$  (0.7093 Å) X-ray source and a CCD Atlas detector at distance 60 mm. Data were collected between  $4$  and  $46.7^\circ 2\theta$  with an exposure time of  $\sim 180$  s. The sample was mounted in a 0.5 mm glass capillary sealed with glue.

*In situ* SR-PXD data for sample **S1** were measured at the beamline BM01A of the Swiss-Norwegian Beam Lines (SNBL), European Synchrotron Radiation Facility (ESRF), Grenoble, France, using a MAR345 image plate detector. The samples were mounted in glass capillaries (o.d. 0.5 mm) sealed with a composite adhesive to prevent contact with air. The data were collected at a sample-to-detector distance of 240 mm and the capillaries were rotated  $20^\circ$  during the data collection. The X-ray

**Table 2**  
The calculated gravimetric hydrogen content,  $\rho_{\text{m}}(\text{H}_2)$ , for LiBH<sub>4</sub>–LiI (1:0.5, **S1**) and a reference sample of as-received LiBH<sub>4</sub> are compared to the measured hydrogen content in four desorption cycles using the Sieverts method. The absorption times are shown for each hydrogenation cycle since this has an impact on the amount of gas released from the sample.

| Samples                        | $\rho_{\text{m}}(\text{H}_2)$ (wt%) | Des1 (wt%) | Abs1 time (h) | Des2 (wt%) | Abs2 time (h) | Des3 (wt%) | Abs3 time (h) | Des4 (wt%) | H <sub>2</sub> uptake (%) |
|--------------------------------|-------------------------------------|------------|---------------|------------|---------------|------------|---------------|------------|---------------------------|
| LiBH <sub>4</sub>              | 13.88                               | 13.2       | 58            | 3.4        | –             | –          | –             | –          | 25                        |
| LiBH <sub>4</sub> –LiI (1:0.5) | 3.40                                | 3.4        | 58            | 2.7        | 64            | 2.6        | 44            | 2.3        | 68                        |

exposure time for each powder pattern was 20 s using a selected wavelength of  $\lambda = 0.709637$  Å. The wavelength and the detector geometry were calibrated using an external standard, LaB<sub>6</sub>. The sample was heated from RT to 300 °C with a heating rate of 5 °C/min and subsequently cooled naturally to 26 °C. This procedure was repeated three consecutive times using the same sample.

*In situ* SR-PXD data were measured for **S1A** and **S4** at the MAX-II synchrotron, beamline 1711 at MAX-lab, Lund, Sweden with a MAR165 CCD detector system ( $\lambda = 0.907700$  and  $0.94608$  Å for **S1A** and **S4**, respectively) [40]. The samples were mounted in sapphire (Al<sub>2</sub>O<sub>3</sub>) single-crystal tubes (1.09 mm o.d., 0.79 mm i.d.) under argon [41,42]. The X-ray exposure time was 30 s per PXD pattern and the samples were heated from RT to 240 °C (**S1A**) or from RT to 280 °C (**S4**). The latter sample was kept at 280 °C for 30 min and then heated from 280 to 290 °C. A heating ramp of 5 °C/min was used for all experiments.

All SR-PXD data were integrated using the Fit2D program [43] and analyzed by Rietveld refinement using FullProf Suite [44]. The background was described by linear interpolation between selected points, while Gauss profile functions were used to fit the diffraction peaks. In the refinements, scale factors, unit cell parameters, profile parameters (*U*, *V*, *W*), the overall temperature factor and the background were refined. The structural model for the solid solution Li(BH<sub>4</sub>)<sub>1–x</sub>I<sub>x</sub> was developed from the structures of *h*-LiBH<sub>4</sub> and  $\beta$ -LiI, which are identical except for a displacement along the *z*-axis. For the solid solution the individual temperature factors, the occupancies and the atomic *z*-parameter for the anion site were additionally refined. Since the temperature factors and the occupancies are correlated, the temperature factors were initially refined with the occupancies fixed to the value of the prepared composition of the sample. Then the temperature factors were fixed and the occupancies were refined. Generally, the Rietveld refinement program tends to underestimate the uncertainty for the calculated occupancies.

Differential scanning calorimetry (DSC) was performed on **S3** and **S4** with a Netzsch STA449C Jupiter instrument from RT to 430 °C with a heating rate of 1.5 °C/min in helium (purity 4.6) atmosphere. The samples were contained in Al<sub>2</sub>O<sub>3</sub> crucibles.

Infrared spectroscopy measurements were performed for **S2A** using an ATR-IR spectrophotometer (Bruker Alpha equipped with an ATR accessory with Ge crystal), placed in an argon-filled glove box.

Sieverts measurements were recorded for **S1** with a PCTpro 2000 instrument from Hy-Energy [45]. The samples were loaded in an autoclave and sealed in argon atmosphere. Temperature-programmed desorption (TPD) experiments were performed in the temperature range RT to 540 °C (0.5 °C/min) in  $p(\text{H}_2) = 1$  bar. Hydrogen absorption data were measured under an initial hydrogen pressure of ca. 100 bar at a temperature of 410 °C for 44–64 h, see Table 2.

## 3. Results and discussion

### 3.1. Investigation of the iodide substitution mechanism by *in situ* SR-PXD

#### 3.1.1. Substitution by mechano-chemical synthesis, ball milling

In order to study the mechanism of the anion substitution, an *in situ* SR-PXD experiment of a ball-milled sample of LiBH<sub>4</sub>–LiI (1:0.5, **S1**), has been performed, see Fig. 1. The sample was heated from RT to 300 °C and cooled to 26 °C. This procedure was repeated three consecutive times. The first diffractogram, measured at 35 °C, contains Bragg reflections from the solid solution *h*-Li(BH<sub>4</sub>)<sub>1–x</sub>I<sub>x</sub>

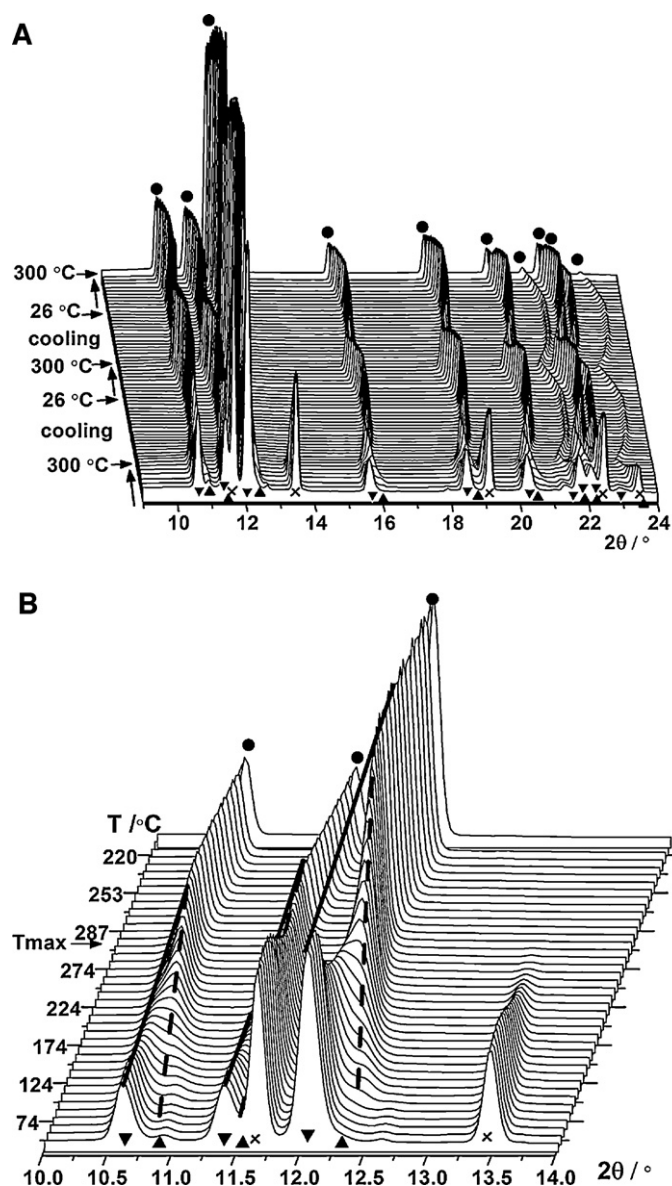


**Fig. 1.** (A) *In situ* SR-PXD data for a ball-milled sample of  $\text{LiBH}_4\text{-LiI}$  (1:0.5, **S1A**) measured at ESRF BM01A. The sample was heated from RT to 300 °C three times and cooled to 26 °C between each consecutive heating (5 °C/min). (B) Enlarged section of the *in situ* SR-PXD data shown in (A) in the  $2\theta$  region 10–14° and temperature region RT to 220 °C of the first heating. Symbols:  $\times$   $\alpha$ -LiI,  $\nabla$   $h\text{-Li}(\text{BH}_4)_{1-x}\text{I}_x$ ,  $\blacktriangle$   $h\text{-Li}(\text{BH}_4)_{1-y}\text{I}_y$ ,  $\bullet$   $h\text{-Li}(\text{BH}_4)_{0.61}\text{I}_{0.39}$  ( $\lambda = 0.709637 \text{ \AA}$ ).

with  $x = 0.67$ ,  $\alpha$ -LiI and weak reflections from  $o\text{-LiBH}_4$  ( $V/Z = 54 \text{ \AA}^3$  as reported for pure  $o\text{-LiBH}_4$  [3]). The occupancies of the anions in the solid solution were determined from Rietveld refinements of the data, see details in Section 2.  $o\text{-LiBH}_4$  transforms at 70 °C to a hexagonal solid solution  $h\text{-Li}(\text{BH}_4)_{1-y}\text{I}_y$  with a lower volume ( $V/Z = 57.1 \text{ \AA}$ ) as compared to  $h\text{-Li}(\text{BH}_4)_{1-x}\text{I}_x$  simultaneously present in the sample ( $V/Z = 60.5 \text{ \AA}$ ). The reflections are initially too weak to reliably determine the iodide content, however, the smaller size of the unit cell suggest a lower iodide content.

Upon further heating the intensity of the  $\alpha$ -LiI Bragg reflections decreases and the two solid solutions  $h\text{-Li}(\text{BH}_4)_{1-x}\text{I}_x$  and  $h\text{-Li}(\text{BH}_4)_{1-y}\text{I}_y$  are merging to become a single solid solution of  $h\text{-Li}(\text{BH}_4)_{0.61}\text{I}_{0.39}$  at 264 °C (see Fig. 1B). The composition was determined by Rietveld refinement, which gave values different from the sample composition. This is due to the strong correlation between the relative occupancies (*i.e.* the  $\text{BH}_4/\text{I}$  ratio) and the temperature factors. The composition remains almost constant during the rest

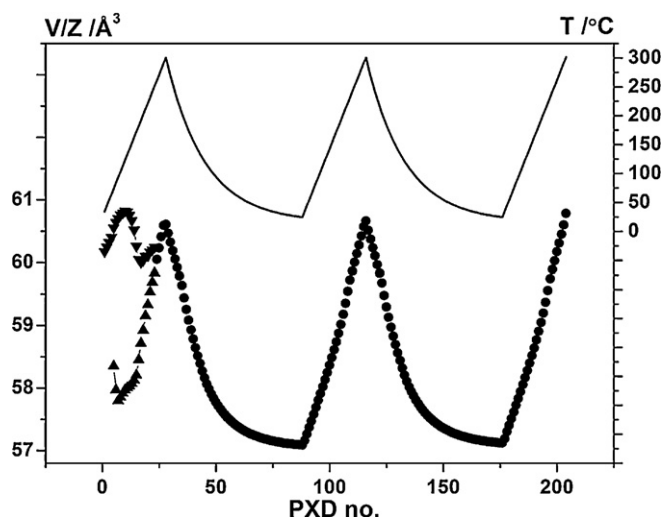


**Fig. 2.** The unit cell volumes per formula unit  $V/Z$  for the two solid solutions  $h\text{-Li}(\text{BH}_4)_{1-x}\text{I}_x$  and  $h\text{-Li}(\text{BH}_4)_{1-y}\text{I}_y$  and the fully substituted sample  $h\text{-Li}(\text{BH}_4)_{0.61}\text{I}_{0.39}$  determined from Rietveld refinements of the data shown in Fig. 1A and plotted as a function of PXD no., while the temperature has been cycled. Notice the formation of two solid solutions at the beginning of the first cycle. Symbols:  $\nabla$   $h\text{-Li}(\text{BH}_4)_{1-x}\text{I}_x$ ,  $\blacktriangle$   $h\text{-Li}(\text{BH}_4)_{1-y}\text{I}_y$ ,  $\bullet$   $h\text{-Li}(\text{BH}_4)_{0.61}\text{I}_{0.39}$ . The solid line shows the corresponding temperature.

of the experiment, *i.e.*  $h\text{-Li}(\text{BH}_4)_{0.61}\text{I}_{0.39}$  is stable from RT to temperatures above 300 °C. Thus, the structure of the solid solution is isostructural to both  $h\text{-LiBH}_4$  and  $\beta\text{-LiI}$  with space group symmetry  $P6_3mc$  [35–37].

A plot of the unit cell volumes for the solid solutions  $\text{Li}(\text{BH}_4)_{1-x}\text{I}_x$  observed during the experiment is shown in Fig. 2. This illustrates the coexistence of two solid solutions denoted  $h\text{-Li}(\text{BH}_4)_{1-x}\text{I}_x$  and  $h\text{-Li}(\text{BH}_4)_{1-y}\text{I}_y$  ( $x > y$ ) with different unit cell volume, *i.e.* different degree of substitution, at the beginning of the experiment. Furthermore, the observation of the similar unit cell volumes at 26 °C after each heating and the linear thermal expansion during the second and third heating suggests that  $\alpha$ -LiI does not segregate from the fully substituted solid solution  $h\text{-Li}(\text{BH}_4)_{0.61}\text{I}_{0.39}$  on the time scale of the experiment. It is also noteworthy that the hexagonal-orthorhombic polymorphic phase transition normally observed at 112 °C for  $\text{LiBH}_4$  [3,31,32,34] is not observed for  $h\text{-Li}(\text{BH}_4)_{1-x}\text{I}_x$  down to RT, suggesting that the substitution stabilizes the hexagonal structure.

### 3.1.2. Anion substitution by thermal treatment

Anion substitution facilitated by thermal treatment was studied using a ball-milled sample of  $\text{LiBH}_4\text{-LiI}$  (1:0.5, **S1A**) annealed at 280 °C for 96 h. SR-PXD data collected at RT reveal a single solid solution of  $h\text{-Li}(\text{BH}_4)_{0.73}\text{I}_{0.27}$  with an iodide content of 27 mol%, see Fig. A in the supplementary information. The iodide content was determined with Rietveld refinement and is found to be similar to the initial sample composition.  $h\text{-Li}(\text{BH}_4)_{0.73}\text{I}_{0.27}$  is observed as a single solid solution during the *in situ* experiment from RT to 280 °C. The annealing was performed 14 days prior to measurement of the SR-PXD data shown in Fig. A in supplementary information.

A sample of  $\text{LiBH}_4\text{-LiI}$  (1:0.6, **S2A**) was investigated 27 months after the annealing and the PXD data shows Bragg reflections from a single solid solution  $h\text{-Li}(\text{BH}_4)_{1-x}\text{I}_x$ , *i.e.* no segregation of LiI and  $o\text{-LiBH}_4$  is observed. However, a small amount ( $\sim 4$  wt%) of a hydrate,  $\text{LiI}\cdot\text{H}_2\text{O}$  is formed, see Fig. B in the supplementary information. The composition of the sample cannot be accurately determined due to insufficient data quality. This shows that the anion substitution facilitated by thermal treatment (annealing) is stable at RT over time, for more than a year.

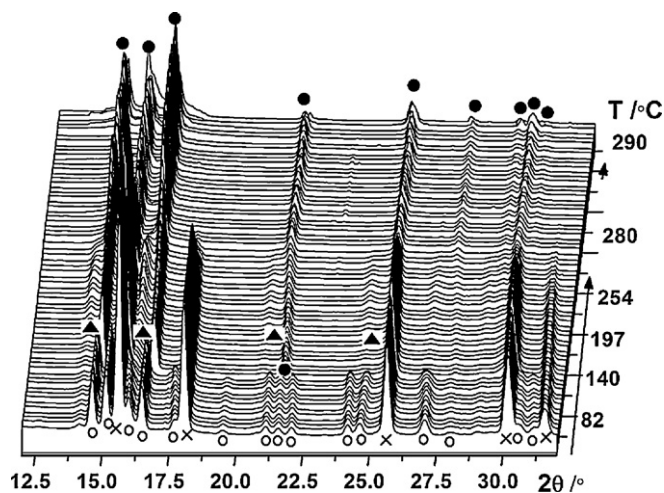


**Fig. 3.** *In situ* SR-PXD data measured at MAX-Lab for a hand-mixed sample of  $\text{LiBH}_4\text{-LiI}$  (1:1, **S4**). The sample was heated from RT to 280 °C, kept at a constant temperature of 280 °C for 30 min, and then heated from 280 to 290 °C (heating rate 5 °C/min). Symbols:  $\times$   $\alpha$ -LiI,  $\circ$   $o$ - $\text{LiBH}_4$ ,  $\bullet$   $h$ - $\text{Li}(\text{BH}_4)_{1-x}\text{I}_x$ ,  $\blacktriangle$   $h$ - $\text{Li}(\text{BH}_4)_{1-y}\text{I}_y$  ( $\lambda = 0.94608 \text{ \AA}$ ).

### 3.1.3. Substitution by hand-mixing in a mortar

A hand-mixed sample of  $\text{LiBH}_4\text{-LiI}$  (1:1, **S4**) has been prepared and investigated using *in situ* SR-PXD measured from RT to 290 °C, see Fig. 3. The first diffractogram, measured at 28 °C, contains Bragg reflections from the starting materials,  $o$ - $\text{LiBH}_4$  and  $\alpha$ -LiI. The polymorphic phase transformation from  $o$ - $\text{LiBH}_4$  to  $h$ - $\text{LiBH}_4$  is observed at 112 °C. Upon further heating the dissolution of LiI into  $h$ - $\text{LiBH}_4$  is observed as a gradual decrease of the intensity of the  $\alpha$ -LiI reflections, followed by formation of a solid solution,  $h$ - $\text{Li}(\text{BH}_4)_{1-x}\text{I}_x$ . Apparently, two solid solutions of  $h$ - $\text{Li}(\text{BH}_4)_{1-x}\text{I}_x$  and  $h$ - $\text{Li}(\text{BH}_4)_{1-y}\text{I}_y$  are in equilibrium as observed for the ball-milled sample **S1**. At  $T = 219$  °C, the two solid solutions obtain iodide substitution degrees of  $\sim 64$  mol% and  $\sim 0$ –5 mol% and unit cell volumes per formula unit of  $61.8 \text{ \AA}^3$  and  $56.1 \text{ \AA}^3$ , respectively. Observation of a larger unit cell volume for the solid solution with higher degree of substitution, agrees well with the larger ionic radii of  $\text{I}^-$  ( $\sim 2.20 \text{ \AA}$ ) as compared to  $\text{BH}_4^-$  ( $\sim 2.03 \text{ \AA}$ ). The reflections from the solid solution  $h$ - $\text{Li}(\text{BH}_4)_{1-y}\text{I}_y$ ,  $y \sim 0$ –5 mol% disappear at  $T = 270$  °C, which is due to formation of a single  $\text{Li}(\text{BH}_4)_{1-x}\text{I}_x$  solid solution as observed for the ball-milled sample **S1**, since the reflections from  $\alpha$ -LiI do not reappear.

There is no indication of iodide substitution in the orthorhombic polymorph of lithium borohydride,  $o$ - $\text{LiBH}_4$  or  $\text{BH}_4^-$  substitution in the cubic  $\alpha$ -LiI in any of the samples. For  $\text{LiBH}_4$  this might be explained by the structural dynamics, *i.e.* the librational motion of the  $\text{BH}_4^-$  complex ion, which is significantly larger for  $h$ - $\text{LiBH}_4$  than for  $o$ - $\text{LiBH}_4$  [31,32]. For LiI, the hexagonal structure is energetically favoured if only the binding energy is considered, furthermore, it has been reported that  $\text{Br}^-$  substitution stabilizes the hexagonal structure of  $\beta$ -LiI up to  $T \sim 80$  °C [35].

Previously, a trend in the structural chemistry of anion substitution in borohydrides with the heavier halides was reported [21]: a smaller anion tends to dissolve into the compound containing the larger anion, and the structure of the latter tends to be preserved in the obtained solid solution. This trend follows the relative size of the anions,  $\text{I}^- > \text{BH}_4^- > \text{Br}^- > \text{Cl}^-$  [46]. This explains that LiCl dissolves in  $\text{LiBH}_4$  while  $\text{LiBH}_4$  does not dissolve in LiCl [20]. However, when two solids have identical structures the dissolution process may produce two solid solutions as observed for  $\text{NaBH}_4\text{-NaCl}$ , where a small amount of  $\text{NaBH}_4$  dissolves in NaCl and a larger amount of NaCl dissolves in  $\text{NaBH}_4$  [47]. The solid solutions found

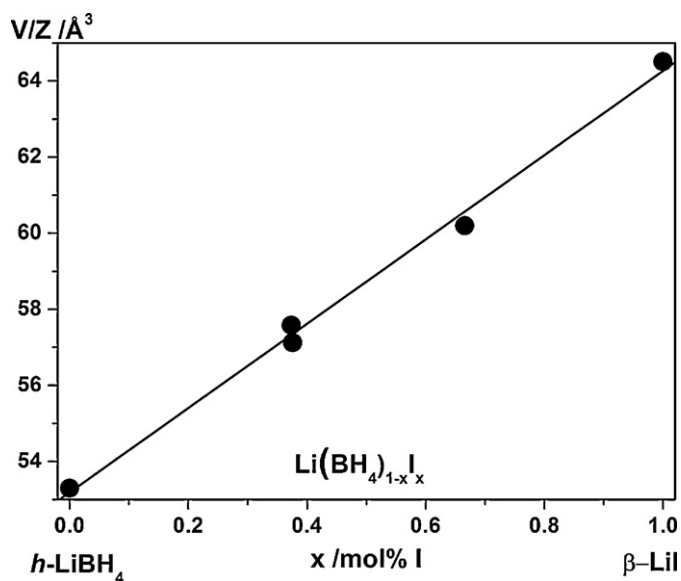


**Fig. 4.** Unit cell volume per formula unit,  $V/Z$  as a function of the composition of  $\text{Li}(\text{BH}_4)_{1-x}\text{I}_x$ . The values are determined from Rietveld refinements of SR-PXD data measured at RT for sample **S1**, see Table A in the supplementary information. The volume of  $h$ - $\text{LiBH}_4$  at 25 °C is estimated from the thermal expansion coefficient ( $2.9 \times 10^{-4} \text{ K}^{-1}$ ) [32] and the volume of  $\beta$ -LiI at 25 °C is given in the literature [35].

in the system  $\text{LiBH}_4\text{-LiI}$  follow the above-mentioned trend since the structures of  $h$ - $\text{LiBH}_4$  and  $\beta$ -LiI are identical.

A linear relation between the unit cell volume and the iodide content,  $x$ , in the observed solid solutions is shown in Fig. 4. The unit cell volume of  $h$ - $\text{LiBH}_4$  at 25 °C has been estimated from the thermal expansion coefficient of  $h$ - $\text{LiBH}_4$ ,  $2.9 \times 10^{-4} \text{ K}^{-1}$ , and the volume of  $\beta$ -LiI at 25 °C is reported in the literature [32,35]. The volumes determined for different compositions of  $\text{Li}(\text{BH}_4)_{1-x}\text{I}_x$  are listed in Table A in the supplementary information. The relationship between the unit cell volume per formula unit  $V/Z$  and composition of  $\text{Li}(\text{BH}_4)_{1-x}\text{I}_x$  and  $\beta$ -LiI is found to be linear and follow Vegard's law [48].

The size difference of the ions or atoms being mixed is a crucial parameter for the formation of solid solutions [49]. For LiI–LiX ( $X = \text{F}, \text{Cl}, \text{Br}$ ) solid solution, a clear correlation between mixing properties and ionic radius of  $X^-$  can be outlined, if the atomic radii of halides for a coordination number equal to 6 are considered:  $r(\text{F}^-) = 1.33 \text{ \AA}$ ,  $r(\text{Cl}^-) = 1.81 \text{ \AA}$ ,  $r(\text{Br}^-) = 1.96 \text{ \AA}$  and  $r(\text{I}^-) = 2.20 \text{ \AA}$  [50]. LiI–LiF binary system shows a complete immiscibility in the solid state, with a eutectic reaction at 413 °C [51]. Because of the immiscibility in the solid state, a positive heat of mixing is expected for this system. Similar behaviour can be observed for LiI–LiCl system [51], but the eutectic temperature is slightly lower (371 °C), suggesting a lower positive enthalpy of mixing. For LiI–LiBr system, the  $\text{Br}^-$  anion size is closer to that of  $\text{I}^-$ , so that the positive enthalpy of mixing is further reduced and an immiscibility gap becomes evident in the solid state, with a critical temperature of 208 °C [51]. For the  $\text{BH}_4^-$  anion, an ionic radius of 2.03 Å has been suggested [52]. So, a significant miscibility is expected for the LiI– $\text{LiBH}_4$  system in the solid state, as evidenced from the obtained results. In fact, solubility of up to about 80% of LiI in  $\text{LiBH}_4$  has been reported recently [27].

The enthalpy of mixing in binary solid solutions is also correlated with the volume mismatch of the constituents [49]. This behaviour applies also for alkali halide solid solutions with the rock salt structure and a second-order correlation has been suggested [49]. The observed linear trend of the volume of the unit cell for the solid solutions as a function of composition (see Fig. 4) suggests that the volume of mixing is close to zero, so that Vegard's

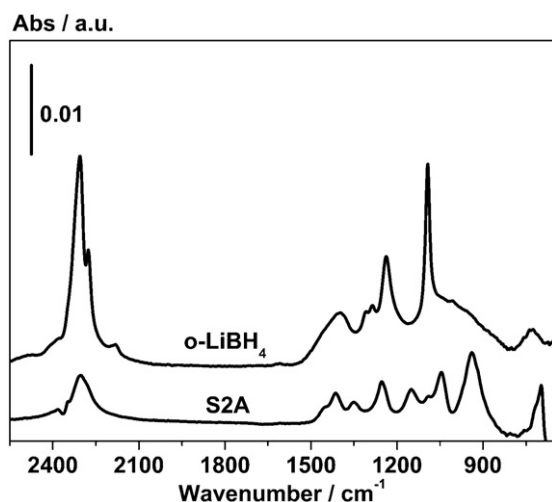


Fig. 5. IR spectra collected in ATR mode (Ge crystal) for  $\text{LiBH}_4$  as received (top) and sample  $\text{LiBH}_4\text{-LiI}$  (1:0.6, **S2A**, bottom).

law is followed by the hexagonal solid solution. As a consequence, a close-to-ideal behaviour is expected for the solution, so that a significant miscibility can be expected in the solid state, because of the entropic contribution. Of course, for the occurrence of a single solid solution it is necessary that any kinetic constraint is overcome by suitable thermal treatments. Therefore, during the experiments, the metastable coexistence of two solid solutions has been found, which becomes a single solid solution after heating (see Fig. 2). For LiI rich solutions, the presence of the cubic structure in the pure component is expected to limit the solubility. A peritectic reaction is likely to occur close to the melting point of LiI (469 °C), but accurate calorimetric measurements are necessary to reach a full picture of the phase diagram.

### 3.2. Infrared spectroscopy of $\text{Li}(\text{BH}_4)_{1-x}\text{I}_x$

In order to study the changes in the vibrational properties of lithium borohydride IR-ATR spectroscopy was performed on an annealed sample of  $\text{LiBH}_4\text{-LiI}$  (1:0.6, **S2A**), see Fig. 5. The IR-ATR spectrum of as-received  $o\text{-LiBH}_4$  shows two main sets of IR absorption bands due to B–H stretching (2400–2000  $\text{cm}^{-1}$  region) and B–H bending (1600–800  $\text{cm}^{-1}$  region) vibrational modes, respectively, as already reported in literature [53–56]. In particular, the Raman spectrum of  $o\text{-LiBH}_4$  at RT has been reported to show a well-defined triplet of bands in the B–H stretching region and a doublet in the B–H bending region [53]. The IR spectrum is more complex in the latter region (as evidenced in Fig. 5), because both IR and Raman active bending modes are observed, as well as bands due to combination and overtones [57]. The vibrational spectra of borohydrides are very sensitive to the geometry of the  $\text{BH}_4^-$  anions. As a consequence, the orthorhombic to hexagonal polymorphic phase transformation in  $\text{LiBH}_4$  leads to a change in the corresponding vibrational spectra, as previously demonstrated by *in situ* Raman spectroscopy measurements as a function of temperature [53]. In particular, upon increasing temperature, the well-defined IR absorption bands in both, B–H stretching and bending regions become gradually less well defined and when the polymorphic phase transformation occurs a single and broad band is observed in both regions.

When  $o\text{-LiBH}_4$  is mixed with  $\alpha\text{-LiI}$  (sample **S2A**) the corresponding IR spectrum shows a significant broadening and a decrease in intensity of the IR absorption bands in the B–H stretching region, which can be explained in terms of a polymorphic phase transformation [53]. Furthermore, the IR spectrum in the low frequency

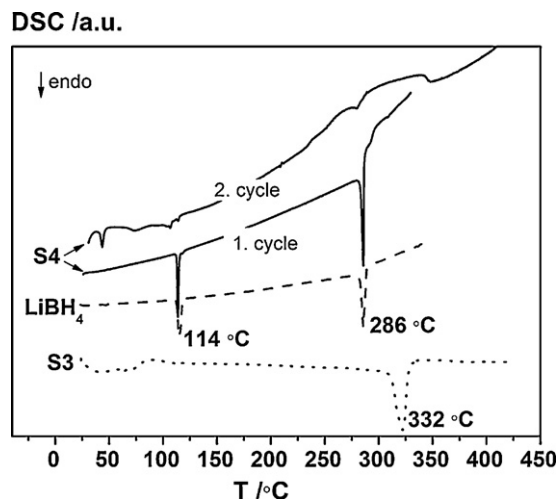


Fig. 6. Differential scanning calorimetry (DSC) conducted from RT to 430 °C (heating rate 1.5 °C/min) for  $\text{LiBH}_4\text{-LiI}$  hand-mixed (1:1, **S4**, solid lines),  $\text{LiBH}_4\text{-LiI}$  ball-milled (1:1, **S3**, dots) and a reference sample of  $\text{LiBH}_4$  (dashes). For  $\text{LiBH}_4\text{-LiI}$  hand-mixed (1:1, **S4**, solid lines) two cycles have been measured and they are marked 1. cycle and 2. cycle in the figure.

region (1500–600  $\text{cm}^{-1}$ ) becomes even more complex than that of the parent  $o\text{-LiBH}_4$ , and reflects a change in the symmetry of the  $\text{BH}_4^-$  anions. Interaction of the  $\text{BH}_4^-$  anions with iodide anions leads to small lattice distortion and disordering effects, thus affecting the vibrational spectrum. Finally, it is worth noting that Li–I vibrational modes cannot be observed in the investigated spectral range, *i.e.* the observed changes are not related to unreacted LiI.

### 3.3. Investigation of the iodide substitution by differential scanning calorimetry

Differential scanning calorimetry (DSC) measurements were conducted for  $\text{LiBH}_4\text{-LiI}$  samples (**S3** and **S4**) and compared with a reference sample of as-received  $\text{LiBH}_4$ . The data are shown in Fig. 6 for the temperature range RT to 430 °C (heating rate 1.5 °C/min). For  $\text{LiBH}_4$  two endothermic peaks are observed in the DSC profile, at 115 and 286 °C, respectively. The first signal corresponds to the polymorphic phase transformation  $o\text{-}$  to  $h\text{-LiBH}_4$  and the second signal to the melting of  $\text{LiBH}_4$  [55]. For the hand-mixed sample of  $\text{LiBH}_4\text{-LiI}$  (**S4**) the DSC profile for the first cycle is similar to that of  $\text{LiBH}_4$  showing two endothermic peaks, at 114 and 286 °C, respectively, in agreement with the SR-PXD data of **S4** shown in Fig. 3. However, during the second cycle, all DSC signals are significantly weakened, indicating the anion substitution has occurred, resulting in formation of the solid solution  $h\text{-Li}(\text{BH}_4)_{1-x}\text{I}_x$ . For the ball-milled  $\text{LiBH}_4\text{-LiI}$  sample (**S3**) one endothermic peak at 322 °C is observed, *i.e.* no signal corresponding to the polymorphic phase transformation from  $o\text{-}$  to  $h\text{-LiBH}_4$  is observed and the melting point is shifted towards higher temperatures compared to  $\text{LiBH}_4$  in agreement with the SR-PXD data shown in Fig. 1.

### 3.4. Hydrogen storage properties of the solid solution $\text{Li}(\text{BH}_4)_{1-x}\text{I}_x$

The hydrogen storage properties of the  $\text{LiBH}_4\text{-LiI}$  system were investigated using the Sieverts method. The four cycles of dehydrogenation for  $\text{LiBH}_4\text{-LiI}$  (1:0.5, **S1**) are measured using a relatively slow heating ramp from RT to 540 °C (0.5 °C/min), see Fig. 7. The first dehydrogenation profile for  $\text{LiBH}_4\text{-LiI}$  (1:0.5, **S1**) is similar to that of  $\text{LiBH}_4$ , *i.e.* the fastest hydrogen release is observed at 450 °C. A total hydrogen release of 3.4 wt% corresponding to the calculated capacity of  $\rho_m(\text{H}_2) = 3.40$  wt% is observed for  $\text{LiBH}_4\text{-LiI}$

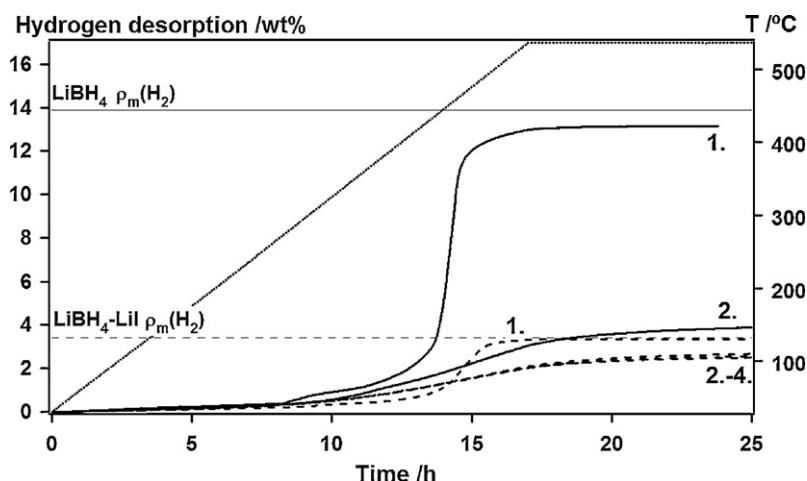


**Fig. 7.** Temperature-programmed desorption measurement using the Sieverts method conducted from RT to 540 °C (heating rate 0.5 °C/min) for LiBH<sub>4</sub> (solid lines, 1. and 2. desorption) and LiBH<sub>4</sub>-LiI ball-milled (1:0.5, **S1**, dashed lines, 1.-4. desorption). The horizontal lines are the calculated hydrogen storage content. The temperature profile is shown as dots.

(1:0.5, **S1**). A total hydrogen release of 13.2 wt% is observed during the first dehydrogenation of LiBH<sub>4</sub>, i.e. 95% of the calculated capacity of  $p(\text{H}_2) = 13.88$  wt%. All hydrogen absorptions were conducted at a constant temperature of 410 °C at  $p(\text{H}_2) = 100$  bar for 44–64 h, see Table 2. The second hydrogen desorption measurement for LiBH<sub>4</sub>-LiI (1:0.5, **S1**) shows a total hydrogen releases of 2.7 wt% (79% of the calculated capacity) in contrast to LiBH<sub>4</sub> which only release 3.4 wt% H<sub>2</sub>, i.e. 25% of the calculated hydrogen storage capacity. A third and a fourth desorption for LiBH<sub>4</sub>-LiI (1:0.5, **S1**) was measured after 64 and 44 h of rehydrogenation, respectively, giving a hydrogen release of 2.6 and 2.3 wt% H<sub>2</sub> (76% and 68% of the calculated capacity). The decrease in hydrogen storage capacity may indicate that the sample is not fully loaded with hydrogen during the absorption, see Table 2.

Interestingly, the rehydrogenation seems to occur at more moderate conditions for the Li(BH<sub>4</sub>)<sub>1-x</sub>I<sub>x</sub> solid solution as compared to LiBH<sub>4</sub> [58]. After four cycles of hydrogen release and uptake the LiBH<sub>4</sub>-LiI sample still maintains 68% of the calculated hydrogen storage capacity. The hydrogen storage capacity of LiBH<sub>4</sub> under identical conditions maintains only 25% of the calculated capacity after two cycles. These results indicate that iodide substitution in LiBH<sub>4</sub> stabilizes the hydrogenated state and thereby facilitates rehydrogenation.

#### 4. Conclusion

Solid solutions of Li(BH<sub>4</sub>)<sub>1-x</sub>I<sub>x</sub> have been obtained by reacting LiBH<sub>4</sub> with α-LiI. The substitution process can be induced by either heat treatment at elevated temperatures of 245 °C or by mechanochemical treatment, i.e. high-energy ball milling. *In situ* powder X-ray diffraction has demonstrated that anion substitution initially forms two solid solutions, which at elevated temperatures merge into one with a degree of substitution of up to 62 mol%. Two solid solutions may occur due to substitution of I<sup>-</sup> for BH<sub>4</sub><sup>-</sup> in LiBH<sub>4</sub> and substitution of BH<sub>4</sub><sup>-</sup> for I<sup>-</sup> in LiI. The structures of the solid solutions are identical to the hexagonal structures of *h*-LiBH<sub>4</sub> and β-LiI. The solid solutions of Li(BH<sub>4</sub>)<sub>1-x</sub>I<sub>x</sub> have a broader stability range (from RT to the melting at 330 °C) as compared to that of both *h*-LiBH<sub>4</sub> and β-LiI. Attenuated infrared spectroscopy reveal interesting features in the low-frequency region and a clear indication of the hexagonal solid solution present at RT in agreement with powder X-ray diffraction and differential scanning calorimetry data. Furthermore, the Sieverts measurements indicate that the rehydrogenation occurs more efficiently for the solid solution

Li(BH<sub>4</sub>)<sub>1-x</sub>I<sub>x</sub> as compared to LiBH<sub>4</sub> possibly due to stabilization of the anion substituted material.

#### Acknowledgements

We gratefully acknowledge the financial support from the European Commission (contract NMP-2008-261/FLYHY), the Danish Research Council for Natural Sciences (Danscatt), the Danish National Research Foundation (Centre for Materials Crystallography), the Danish Strategic Research Council (Centre for Energy Materials) and the Carlsberg Foundation. The authors finally acknowledge the Swiss-Norwegian Beam Lines (SNBL), European Synchrotron Radiation Facility (ESRF), Grenoble, France and the MAX-II synchrotron facility at the research laboratory MAX-lab, Lund, Sweden for the allocated beam time.

#### Appendix A. Supplementary data

Supplementary data associated with this article can be found, in the online version, at doi:10.1016/j.jallcom.2011.05.031.

#### References

- [1] U. Eberle, M. Felderhoff, F. Schüth, *Angew. Chem. Int. Ed.* 48 (2009) 6608–6630.
- [2] J. Graetz, *Chem. Soc. Rev.* 38 (2009) 73–82.
- [3] J.P. Soulie, G. Renaudin, R. Cerny, K. Yvon, *J. Alloys Compd.* 346 (2002) 200–205.
- [4] L. Schlapbach, A. Züttel, *Nature* 414 (2001) 353–358.
- [5] Y. Filinchuk, D. Chernyshov, V. Dmitriev, *Z. Kristallogr.* 223 (2008) 649–659.
- [6] A. Züttel, A. Borgschulte, S.I. Orimo, *Scr. Mater.* 56 (2007) 823–828.
- [7] H.W. Li, S.I. Orimo, Y. Nakamori, K. Miwa, N. Ohba, S. Towata, A. Züttel, *J. Alloys Compd.* 446–447 (2007) 315–318.
- [8] H. Hagemann, M. Longhini, J.W. Kaminski, T.A. Wesolowski, R. Cerny, N. Penin, M.H. Sørbj, B.C. Hauback, G. Severa, C.M. Jensen, *J. Phys. Chem. A* 112 (2008) 7551–7555.
- [9] R. Cerny, G. Severa, D.B. Ravnsbæk, Y. Filinchuk, V. d'Anna, H. Hagemann, D. Haase, C.M. Jensen, T.R. Jensen, *J. Phys. Chem. C* 114 (2010) 1357–1364.
- [10] D.B. Ravnsbæk, Y. Filinchuk, Y. Cerenius, H.J. Jakobsen, F. Besenbacher, J. Skibsted, T.R. Jensen, *Angew. Chem. Int. Ed.* 48 (2009) 6659–6663.
- [11] L. Seballos, J.Z. Zhang, E. Rönnebro, J.L. Herberg, E.H. Majzoub, *J. Alloys Compd.* 476 (2009) 446–450.
- [12] D.B. Ravnsbæk, Y. Filinchuk, R. Cerny, T.R. Jensen, *Z. Kristallogr.* 225 (2010) 557–569.
- [13] L.H. Rude, T.K. Nielsen, D.B. Ravnsbæk, U. Bösenberg, M.B. Ley, B. Richter, L.M. Arnbjerg, M. Dornheim, Y. Filinchuk, F. Besenbacher, T.R. Jensen, *Phys. Status Solidi B* (2011) (Accepted).
- [14] J.Y. Lee, D. Ravnsbæk, Y. Lee, Y. Kim, Y. Cerenius, J. Shim, T.R. Jensen, N.H. Hur, Y.W. Cho, *J. Phys. Chem. C* 113 (2009) 15080–15086.
- [15] U. Bösenberg, S. Doppiu, L. Mosegaard, G. Barkhordarian, N. Eigen, A. Borgschulte, T.R. Jensen, Y. Cerenius, O. Gutfleisch, T. Klassen, M. Dornheim, R. Bormann, *Acta Mater.* 55 (2007) 3951–3958.

- [16] U. Bösenberg, J.W. Kim, D. Gosslar, N. Eigen, T.R. Jensen, J.M. von Colbe, Y. Zhou, M. Dahms, D.H. Kim, R. Günther, Y.W. Cho, K.H. Oh, T. Klassen, R. Bormann, M. Dornheim, *Acta Mater.* 58 (2010) 3381–3389.
- [17] Y.W. Cho, J. Shim, B. Lee, *Calphad* 30 (2006) 65–69.
- [18] T.K. Nielsen, U. Bosenberg, R. Goslawit, M. Dornheim, Y. Cerenius, F. Besenbacher, T.R. Jensen, *ACS Nano* 4 (2010) 3903–3908.
- [19] T.K. Nielsen, F. Besenbacher, T.R. Jensen, *Nanoscale* 3 (2011) 2086–2098.
- [20] L.M. Arnbjerg, D.B. Ravnsbæk, Y. Filinchuk, R.T. Vang, Y. Cerenius, F. Besenbacher, J.E. Jørgensen, H.J. Jakobsen, T.R. Jensen, *Chem. Mater.* 21 (2009) 5772–5782.
- [21] L.H. Rude, Y. Filinchuk, M.H. Sørby, B.C. Hauback, F. Besenbacher, T.R. Jensen, *J. Phys. Chem. C* 115 (2011) 7768–7777.
- [22] J.Y. Lee, Y. Lee, J. Suh, J. Shim, Y.W. Cho, *J. Alloys Compd.* 506 (2010) 721–727.
- [23] L. Mosegaard, B. Møller, J. Jørgensen, Y. Filinchuk, Y. Cerenius, J.C. Hanson, E. Dimasi, F. Besenbacher, T.R. Jensen, *J. Phys. Chem. C* 112 (2008) 1299–1303.
- [24] M. Corno, E. Pinatel, P. Ugliengo, M. Baricco, *J. Alloys Compd.* (2010), doi:10.1016/j.jallcom.2010.10.005.
- [25] H. Maekawa, M. Matsuo, H. Takamura, M. Ando, Y. Noda, T. Karahashi, S. Orimo, *J. Am. Chem. Soc.* 131 (2009) 894–895.
- [26] M. Matsuo, H. Takamura, H. Maekawa, H. Li, S.I. Orimo, *Appl. Phys. Lett.* 94 (2009) 084103.
- [27] A. Borgschulte, R. Gremaud, S. Kato, N.P. Stadie, A. Remhof, A. Züttel, M. Matsuo, S.I. Orimo, *Appl. Phys. Lett.* 97 (2010) 031916.
- [28] H. Oguchi, M. Matsuo, J.S. Hummelshøj, T. Vegge, J.K. Nørskov, T. Sato, Y. Miura, H. Takamura, H. Maekawa, S.I. Orimo, *Appl. Phys. Lett.* 94 (2009) 141912.
- [29] M. Matsuo, T. Sato, Y. Miura, H. Oguchi, Y. Zhou, H. Maekawa, H. Takamura, S.I. Orimo, *Chem. Mater.* 22 (2010) 2702–2704.
- [30] M. Matsuo, A. Remhof, P. Martelli, R. Caputo, M. Ernst, Y. Miura, T. Sato, H. Oguchi, H. Maekawa, H. Takamura, A. Borgschulte, A. Züttel, S.I. Orimo, *J. Am. Chem. Soc.* 131 (2009) 16389–16391.
- [31] M.R. Hartman, J.J. Rush, T.J. Udovic, R.C. Bowman Jr., S.J. Hwang, *J. Solid State Chem.* 180 (2007) 1298–1305.
- [32] Y. Filinchuk, D. Chernyshov, R. Cerny, *J. Phys. Chem. C* 112 (2008) 10579–10584.
- [33] Y. Filinchuk, D. Chernyshov, A. Nevidomskyy, V. Dmitriev, *Angew. Chem. Int. Ed.* 47 (2008) 529–532.
- [34] V. Dmitriev, Y. Filinchuk, D. Chernyshov, A.V. Talyzin, A. Dzwilewski, O. Andersson, B. Sundqvist, A. Kurnosov, *Phys. Rev. B* 77 (2008) 174112.
- [35] D. Fischer, A. Müller, M. Jansen, *Z. Anorg. Allg. Chem.* 630 (2004) 2697–2700.
- [36] B. Wassermann, W. Hönle, T.P. Martin, *Solid State Commun.* 65 (1988) 561–564.
- [37] W. Rühl, *Z. Phys.* 143 (1956) 591–604.
- [38] D.C. Johnson, *Nature* 454 (2008) 174–175.
- [39] Y. Liebold-Ribeiro, D. Fischer, M. Jansen, *Angew. Chem. Int. Ed.* 47 (2008) 4428–4431.
- [40] Y. Cerenius, K. Stahl, L.A. Svensson, T. Ursby, A. Oskarsson, J. Albertsson, A. Liljas, *J. Synchrotron Radiat.* 7 (2000) 203–208.
- [41] L. Mosegaard, B. Møller, J.E. Jørgensen, U. Bösenberg, M. Dornheim, J.C. Hanson, Y. Cerenius, G.S. Walker, H.J. Jakobsen, F. Besenbacher, T.R. Jensen, *J. Alloys Compd.* 446–447 (2007) 301–305.
- [42] T.R. Jensen, T.K. Nielsen, Y. Filinchuk, J.E. Jørgensen, Y. Cerenius, E.M. Gray, C.J. Webb, *J. Appl. Crystallogr.* 43 (2010) 1456–1463.
- [43] A.P. Hammersley, S.O. Svensson, M. Hanfland, A.N. Fitch, D. Hausermann, *High Pressure Res.* 14 (1996) 235–248.
- [44] J. Rodriguez-Carvajal, Fullprof Suite, LLB Sacley & LCSIM Rennes, France, 2003.
- [45] PCTPro-2000, Calorimetry and Thermal Analysis, <http://www.setaram.com/PCTPro-2000.htm>, 2011.
- [46] Y. Filinchuk, H. Hagemann, *Eur. J. Inorg. Chem.* 20 (2008) 3127–3133.
- [47] D.B. Ravnsbæk, L.H. Rude, T.R. Jensen, *J. Solid State Chem.* (2011), doi:10.1016/j.jssc.2011.05.030.
- [48] L.Z. Vegard, *Phys. A: Hadrons Nucl.* 5 (1921) 17–26.
- [49] P.K. Davies, A. Navrotsky, *J. Solid State Chem.* 46 (1983) 1–22.
- [50] R.D. Shannon, *Acta Crystallogr. A* 32 (1976) 751–767.
- [51] FACT Sage Database, [www.crct.polymtl.ca/Fact](http://www.crct.polymtl.ca/Fact), 2011.
- [52] C.W.F.T. Pistorius, *Z. Phys. Chem., Neue Folge* 88 (1974) 253.
- [53] S. Gomes, H. Hagemann, K. Yvon, *J. Alloys Compd.* 346 (2002) 206–210.
- [54] S.I. Orimo, Y. Nakamori, J.R. Eliseo, A. Züttel, C.M. Jensen, *Chem. Rev.* 107 (2007) 4111–4132.
- [55] S.I. Orimo, Y. Nakamori, A. Züttel, *Mater. Sci. Eng. B* 108 (2004) 51–53.
- [56] H. Hagemann, Y. Filinchuk, D. Chernyshov, W. Van Beek, *Phase Transitions* 82 (2009) 344–355.
- [57] K.B. Harvey, N.R. McQuaker, *Can. J. Chem.* 49 (1971) 3282–3286.
- [58] A. Züttel, P. Wenger, S. Rentsch, P. Sudan, P. Mauron, C. Emmenegger, *J. Power Sources* 118 (2003) 1–7.